

# Robust photon-spin entangling gate using a quantum-dot spin in a microcavity

C.Y. Hu<sup>1,\*</sup>, W.J. Munro<sup>2,3</sup>, J.L. O'Brien<sup>1</sup>, and J.G. Rarity<sup>1</sup>

<sup>1</sup>*Department of Electrical and Electronic Engineering,*

*University of Bristol, University Walk, Bristol BS8 1TR, United Kingdom*

<sup>2</sup>*Hewlett-Packard Laboratories, Filton Road, Stoke Gifford, Bristol BS34 8QZ, United Kingdom and*

<sup>3</sup>*National Institute of Informatics, 2-1-2 Hitotsubashi, Chiyoda-ku, Tokyo 101-8430, Japan*

(Dated: November 4, 2018)

Semiconductor quantum dots (known as artificial atoms) hold great promise for solid-state quantum networks and quantum computers. To realize a quantum network, it is crucial to achieve light-matter entanglement and coherent quantum-state transfer between light and matter. Here we present a robust photon-spin entangling gate with high fidelity and high efficiency (up to 50 percent) using a charged quantum dot in a double-sided microcavity. This gate is based on giant circular birefringence induced by a single electron spin, and functions as an optical circular polariser which allows only one circularly-polarized component of light to be transmitted depending on the electron spin states. We show this gate can be used for single-shot quantum non-demolition measurement of a single electron spin, and can work as an entanglement filter to make a photon-spin entangler, spin entangler and photon entangler as well as a photon-spin quantum interface. This work allows us to make all building blocks for solid-state quantum networks with single photons and quantum-dot spins.

## I. INTRODUCTION

A quantum network<sup>1</sup> utilizes matter quantum bits (qubits) to store and process quantum information at local nodes, and light qubits (photons) for long-distance quantum state transmission between different nodes. Quantum networks can be used for distributed quantum computing or for large scale and long distance quantum communications between spatially remote parties. There are several physical systems based on cavity quantum electrodynamics (cavity-QED), which could be used for quantum networks with high success probability for quantum-state transfer or processing. One is the atom-cavity system in which single photon sources<sup>2,3,4</sup>, light-atom entanglement<sup>5,6</sup> and a single-photon single-atom quantum interface<sup>7</sup> have been recently demonstrated. But it is far from a trivial task to scale up and to trap the atoms. Another one is the superconducting qubit-cavity system which attracts great interest in recent years. Single photon generation in the microwave frequency region<sup>8</sup> and a quantum bus allowing distant qubits to interact at will<sup>9,10</sup> have been implemented recently in this system.

The third one is the semiconductor quantum dot (QD)-cavity system<sup>11,12,13,14,15</sup>. Firstly, triggered single-photon sources or polarization-entangled photon pair sources based on semiconductor QDs have been demonstrated with high quantum efficiency, high photon indistinguishability, and low multi-photon emission probability<sup>16,17,18,19,20</sup>. These deterministic photon sources are key ingredients for secure quantum networks. Secondly, semiconductor QD spins are promising candidates to construct qubits for storing and processing quantum states<sup>21,22</sup> due to the long electron spin coherence time ( $T_2 \sim \mu\text{s}$ )<sup>23,24</sup> and spin relaxation time ( $T_1 \sim \text{ms}$ )<sup>25</sup>. Moreover, self-assembled QDs can be embedded in various high-finesse optical microcavities or nanocavities, so cavity-QED can be exploited to engineer QD emissions

or related optical transitions as demanded<sup>26,27,28,29,30,31</sup>. The most attractive feature is its compatibility with standard semiconductor processing techniques. Therefore, the QD-cavity system holds great promise for compact and scalable solid-state quantum networks and quantum computers. However, the photon-spin entanglement and quantum state transfer between photon and QD spin have not yet been demonstrated<sup>14,32</sup>.

Here we propose a robust photon-spin entangling gate using a charged QD in a double-sided microcavity, and show this gate can be used as photon-spin entangler, spin entangler, photon entangler as well as reversible and coherent quantum-state transfer between single photons and QD spins. This gate is based on giant circular birefringence induced by a single electron spin, and is ideal for an optical quantum non-demolition (QND) measurement of a single electron spin in a double-sided microcavity. This gate is robust and flexible compared to our previous gate using a charged QD in a single-sided microcavity<sup>33,34</sup>.

The paper is organized as follows: In Sec. II, the photon-spin entangling gate is introduced. In Sec. III we show this gate can be used for single-shot QND measurements of a single QD spin. After that, we show a spin entangler in Sec. IV, a photon entangler in Sec. V and a photon-spin quantum interface in Sec. VI by applying this photon-spin entangling gate. Finally, we present our conclusions and outlook in Sec. VII.

## II. PHOTON-SPIN ENTANGLING GATE

We consider a singly charged QD, e.g., a self-assembled In(Ga)As QD or a GaAs interfacial QD, or even a semiconductor nanocrystal inside an optical cavity, such as a micropillar or microdisk microcavity, or a photonic crystal nanocavity. Fig. 1a shows a micropillar microcavity

where the two GaAs/Al(Ga)As distributed Bragg reflectors (DBR) and the transverse index guiding provide the three-dimensional confinement of light. The two DBRs are made symmetric in order to achieve high resonant transmission of light. Both DBRs are partially reflective allowing light into and out of the cavity (i.e., a double-sided cavity). The circular cross section of the micropillar supports the circularly polarized light. The QD is located at the antinodes of the cavity field to achieve optimized light-matter coupling.

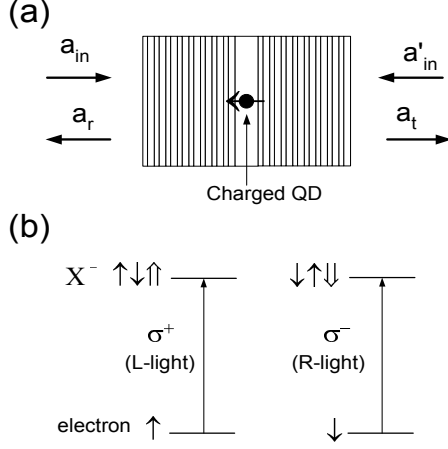


FIG. 1: (a) A charged QD inside a micropillar microcavity with circular cross section. (b) Spin selection rule for optical transitions of negatively-charged exciton  $X^-$  (see text).

The optical properties of singly charged QDs are dominated by the optical resonances of the negatively-charged exciton  $X^-$  (also called trion) which consists of two electrons bound to one hole<sup>35</sup>. Due to the Pauli's exclusion principle,  $X^-$  shows spin-dependent optical transitions (see Fig. 1b)<sup>36</sup>: the left circularly polarized photon (marked by  $|L\rangle$  or L-photon) only couples the electron in the spin state  $|\uparrow\rangle$  to  $X^-$  in the spin state  $|\uparrow\downarrow\uparrow\rangle$  with the two electron spins antiparallel; the right circularly polarized photon (marked by  $|R\rangle$  or R-photon) only couples the electron in the spin state  $|\downarrow\rangle$  to  $X^-$  in the spin state  $|\downarrow\downarrow\downarrow\rangle$ . Here  $|\uparrow\rangle$  and  $|\downarrow\rangle$  represent electron spin states  $|\pm\frac{1}{2}\rangle$ ,  $|\uparrow\rangle$  and  $|\downarrow\rangle$  represent heavy-hole spin states  $|\pm\frac{3}{2}\rangle$ . The light-hole sub-band and the split-off sub-band are energetically far apart from the heavy-hole sub-band and can be neglected. The spin is quantized along the normal direction of the cavity, i.e., the propagation direction of the input (or output) light. This spin selection rule for  $X^-$  is also called the Pauli blocking effect<sup>13,35</sup>.

The reflection and transmission coefficients of this  $X^-$ -cavity structure can be investigated by solving the Heisenberg equations of motion for the cavity field operator  $\hat{a}$  and  $X^-$  dipole operator  $\sigma_-$ , and the input-output

equations<sup>37</sup>:

$$\begin{cases} \frac{d\hat{a}}{dt} = -[i(\omega_c - \omega) + \kappa + \frac{\kappa_s}{2}] \hat{a} - g\sigma_- \\ \quad - \sqrt{\kappa}\hat{a}_{in} - \sqrt{\kappa}\hat{a}'_{in} + \hat{H} \\ \frac{d\sigma_-}{dt} = -[i(\omega_{X^-} - \omega) + \frac{\gamma}{2}] \sigma_- - g\sigma_z\hat{a} + \hat{G} \\ \hat{a}_r = \hat{a}_{in} + \sqrt{\kappa}\hat{a} \\ \hat{a}_t = \hat{a}'_{in} + \sqrt{\kappa}\hat{a} \end{cases} \quad (1)$$

where  $\omega$ ,  $\omega_c$ , and  $\omega_{X^-}$  are the frequencies of the input photon, cavity mode, and  $X^-$  transition, respectively.  $g$  is the  $X^-$ -cavity coupling strength given by  $g = (e^2 f / 4\epsilon_r \epsilon_0 m_0 V_{eff})^{1/2}$  where  $f$  is the  $X^-$  oscillator strength and  $V_{eff}$  is the effective modal volume,  $\gamma/2$  is the  $X^-$  dipole decay rate, and  $\kappa$ ,  $\kappa_s/2$  are the cavity field decay rate into the input/output modes, and the leaky modes, respectively. The background absorption can also be included in  $\kappa_s/2$ .  $\hat{H}$ ,  $\hat{G}$  are the noise operators related to reservoirs.  $\hat{a}_{in}$ ,  $\hat{a}'_{in}$  and  $\hat{a}_r$ ,  $\hat{a}_t$  are the input and output field operators.

In the approximation of weak excitation, i.e., less than one photon inside the cavity per cavity lifetime so that QD is in the ground state at most time, we take  $\langle\sigma_z\rangle \approx -1$ . The reflection and transmission coefficients in the steady state can be obtained

$$\begin{aligned} r(\omega) &= 1 + t(\omega) \\ t(\omega) &= \frac{-\kappa[i(\omega_{X^-} - \omega) + \frac{\gamma}{2}]}{[i(\omega_{X^-} - \omega) + \frac{\gamma}{2}][i(\omega_c - \omega) + \kappa + \frac{\kappa_s}{2}] + g^2}. \end{aligned} \quad (2)$$

By taking  $g = 0$ , we get the reflection and transmission coefficients for an empty cavity where the QD does not couple to the cavity

$$\begin{aligned} r_0(\omega) &= \frac{i(\omega_c - \omega) + \frac{\kappa_s}{2}}{i(\omega_c - \omega) + \kappa + \frac{\kappa_s}{2}} \\ t_0(\omega) &= \frac{-\kappa}{i(\omega_c - \omega) + \kappa + \frac{\kappa_s}{2}} \end{aligned} \quad (3)$$

The reflection and transmission spectra versus the frequency detuning  $\omega - \omega_c$  are presented in Fig. 2a for different coupling strength  $g$ . With increasing  $g$  (e.g. by reducing the effective modal volume  $V_{eff}$ ), the cavity mode splits into two peaks due to the quantum interference in the ‘‘one dimensional atom’’ regime with  $\kappa < 4g^2/\kappa < \gamma$ <sup>38,39</sup> (which has been experimentally demonstrated recently<sup>40</sup>), and the vacuum Rabi splitting in the strong coupling regime with  $g > (\kappa, \gamma)$ <sup>26,27,28,29,30,31</sup>. We notice that the transmittance or reflectance are different between the empty cavity ( $g = 0$ ) and the coupled cavity ( $g \neq 0$ ) (the coupled  $X^-$ -cavity system is called coupled cavity hereafter). This enables us to make a photon-spin entangling gate as discussed below.

If the single excess electron in the QD lies in the spin state  $|\uparrow\rangle$ , the L-photon feels a coupled cavity with reflectance  $|r(\omega)|$  and the transmittance  $|t(\omega)|$ , whereas the R-photon feels the empty cavity with the reflectance  $|r_0(\omega)|$  and transmittance  $|t_0(\omega)|$ ; Conversely, if the electron lies in the spin state  $|\downarrow\rangle$ , the R-photon feels a coupled cavity, whereas the L-photon feels the empty cavity. The difference in transmission and reflection between

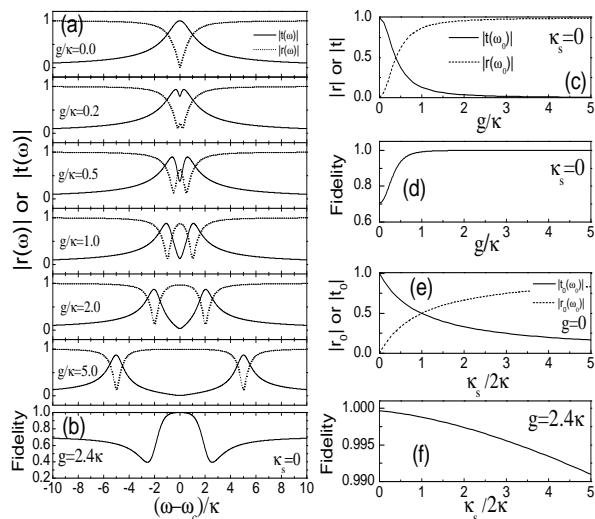


FIG. 2: Calculated transmission and reflection spectra of the  $X^-$ -cavity system. (a) Transmission (solid curves) and reflection (dotted curves) spectra vs the frequency detuning  $(\omega - \omega_c)/\kappa$  for different coupling strength. (b) The gate fidelity vs the frequency detuning in the strong coupling regime ( $g = 2.4\kappa$  is taken). High fidelity can be achieved if  $|\omega - \omega_c| < \kappa < g$ . (c) Transmittance  $|t(\omega_0)|$  (solid curve) and reflectance  $|r(\omega_0)|$  (dotted curve) vs the normalized coupling strength. (d) The gate fidelity vs the normalized coupling strength. (e) Transmittance  $|t(\omega_0)|$  (solid curve) and reflectance  $|r(\omega_0)|$  (dotted curve) vs the normalized side leakage rate. (f) The gate fidelity vs the normalized side leakage rate.  $\omega_c = \omega_{X^-} = \omega_0$  is assumed for (a)-(f).  $\kappa_s = 0$  and  $\gamma = 0.1\kappa$  are taken for (a)-(d).

right and left circularly polarized light, which can be called giant circular birefringence, means we have created a circular polariser controlled by the electron spin. For any quantum input we can define a transmission operator

$$\hat{t}(\omega) = t_0(\omega)(|R\rangle\langle R| \otimes |\uparrow\rangle\langle\uparrow| + |L\rangle\langle L| \otimes |\downarrow\rangle\langle\downarrow|) + t(\omega)(|R\rangle\langle R| \otimes |\downarrow\rangle\langle\downarrow| + |L\rangle\langle L| \otimes |\uparrow\rangle\langle\uparrow|), \quad (4)$$

where  $t_0(\omega)$ ,  $t(\omega)$  are the transmission coefficients of the empty cavity and coupled cavity, respectively.

In the strong coupling regime, i.e.,  $g > (\kappa, \gamma)$  and in the central frequency regime  $|\omega - \omega_c| \ll g$ , we have  $|t(\omega)| \rightarrow 0$  (see Fig. 2a), thus the transmission operator can be simplified as

$$\hat{t}(\omega) \simeq t_0(\omega)(|R\rangle\langle R| \otimes |\uparrow\rangle\langle\uparrow| + |L\rangle\langle L| \otimes |\downarrow\rangle\langle\downarrow|). \quad (5)$$

Obviously, this transmission operator is now constructed from the empty cavity only. We show later how this operator can be used as a photon-spin entangling gate. Here however we can define an operator fidelity (based on amplitude) from equations (4) and (5) as

$$F = \frac{|t_0(\omega)|}{\sqrt{|t_0(\omega)|^2 + |t(\omega)|^2}}. \quad (6)$$

Near-unity fidelity is reached when  $|t(\omega)| \rightarrow 0$  which is only achieved within a small frequency window  $|\omega - \omega_c| < \kappa$  (see Fig. 2b) and in the strong coupling regime with  $g > (\kappa, \gamma)$  (see Fig. 2c and Fig. 2d). The strongly coupled QD-cavity has been demonstrated in various microcavities and nanocavities recently<sup>26,27,28,29,30,31</sup>. For micropillars with diameter around  $1.5 \mu\text{m}$ , the coupling strength  $g = 80 \mu\text{eV}$  and the quality factor more than  $4 \times 10^4$  (corresponding to  $\kappa = 33 \mu\text{eV}$ ) have been reported<sup>26,31</sup>, indicating  $g/\kappa = 2.4$  is achievable for the In(Ga)As QD-cavity system.  $\gamma$  is about several  $\mu\text{eV}$ . Our calculations in Fig. 2 are based on these experimental parameters.

A practical optical cavity can have some side leakage, which induces a decrease in the transmittance of the empty cavity and the gate fidelity (see Fig. 3e and Fig. 3f). However, the improvement of fabrication techniques can suppress the side leakage<sup>31</sup>. When the side leakage is made negligible compared with the main cavity decay into the input/output modes, we get  $|t_0(\omega_0)| = 1$  and unity gate fidelity.

For a realistic QD, the spin selection rule discussed earlier is not perfect if we take the heavy-light hole mixing into account. This can reduce the gate fidelity by a few percent as the hole mixing in the valence band is in the order of a few percent<sup>13,41</sup> [e.g., for self-assembled In(Ga)As QDs]. The hole mixing could be reduced by engineering the shape and size of QDs or using different types of QDs.

As discussed above, the photon-spin entangling gate requires the weak excitation condition, i.e., the input light intensity has to be less than one photon per cavity lifetime. This condition can be satisfied by single photons, e.g. QD single photon sources which can be triggered electrically or optically<sup>16,17,18</sup>. Recently there are lots of experimental efforts to develop high-quality QD single-photon sources with high efficiencies, small multi-photon events and time-bandwidth limited photon pulses<sup>42</sup>.

This photon-spin entangling gate can also work in the reflection geometry, but its application is more complicated and we leave the discussions elsewhere. As a result, the photon-spin entangling gate in the transmission geometry is only 50% efficient.

In the following, we show that this photon-spin entangling gate can be used for QND measurement of a single electron spin, and also can work as photon-spin entangler, spin entangler, or photon entangler. With this gate, reversible quantum state transfer between photon and spin can be implemented. Compared with our previous gate<sup>33,34</sup> and Turchette et al's conditional phase shift gate using a single-sided cavity<sup>43</sup>, this photon-spin entangling gate using a double-sided cavity is more robust and flexible. We notice that other photon-spin entangling gates was also reported recently<sup>32,33,34,44</sup>.

### III. SINGLE-SHOT OPTICAL QND MEASUREMENT OF A SINGLE SPIN

If we prepare the input photon in a linear polarization state  $|H\rangle = (|R\rangle + |L\rangle)/\sqrt{2}$  and the electron spin in the state  $|\psi^s\rangle = |\uparrow\rangle$ , according to equation (5) the state transformation is

$$|H\rangle \otimes |\uparrow\rangle \xrightarrow{\hat{t}(\omega)} \frac{t_0(\omega)}{\sqrt{2}} |R\rangle |\uparrow\rangle. \quad (7)$$

So only the right-handed circularly polarized component is transmitted (see Fig. 3a). Similarly, if the electron spin is in the state  $|\downarrow\rangle$ , only the left-handed circularly polarized component is transmitted (see Fig. 3b). Obviously, this is a circular polariser which allows only one circular polarized light to be transmitted depending on the spin state. This feature enables us to detect the electron spin by measuring the helicity of the transmitted light using a  $\lambda/4$  wave plate and a polarizing beam splitter (see Fig. 3c).

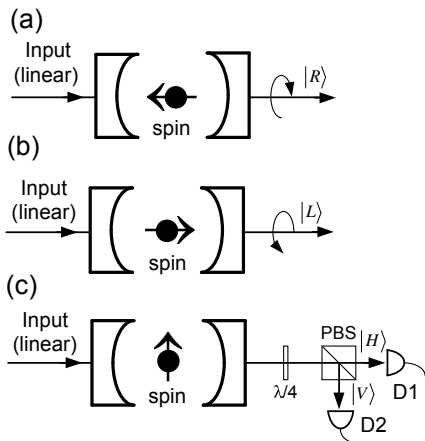


FIG. 3: QND measurement of a single QD spin. (a) The right-circularly polarized component of a linearly polarized light is transmitted if the electron spin in the  $|\uparrow\rangle$  state. (b) The left-circularly polarized component of a linearly polarized light is transmitted if the electron spin in the  $|\downarrow\rangle$  state. (c) Both the right- and left-circularly polarized component of a linearly polarized light are transmitted if the electron spin in a superposition state. PBS (polarizing beam splitter), D1 and D2 (photon detectors), and  $\lambda/4$  (quarter-wave plate).

If the electron spin is in an arbitrary superposition state  $|\psi^s\rangle = \alpha|\uparrow\rangle + \beta|\downarrow\rangle$  (see Fig. 3c), the state transformation is

$$|H\rangle \otimes (\alpha|\uparrow\rangle + \beta|\downarrow\rangle) \xrightarrow{\hat{t}(\omega)} \frac{t_0(\omega)}{\sqrt{2}} (\alpha|R\rangle|\uparrow\rangle + \beta|L\rangle|\downarrow\rangle). \quad (8)$$

Thus after transmission, the light polarization state becomes entangled with the spin state. This is why we call this gate a photon-spin entangling gate. If we measure the light in  $|R\rangle$  (or  $|L\rangle$ ) polarization, the electron spin collapses to  $|\uparrow\rangle$  (or  $|\downarrow\rangle$ ) state. Although this gate

work in the near resonance region, the weak excitation condition means nearly no real excitation occurs in the  $X^-$ -cavity system. As a result, the disturbance to the electron spin system due to the light input is quite small. Within the spin relaxation time ( $\sim$ ms)<sup>25</sup>, repeated measurements will yield the same results, so this single-shot spin detection method is a QND measurement<sup>45</sup>, in contrast to other single-spin detection methods by the time-averaged Faraday rotation or Kerr rotation measurement reported recently<sup>46,47</sup>. In parallel, a QND measurement of single photon polarization state could also be implemented using the above spin QND measurement. QND measurement is critical for scalable quantum information processing<sup>48,49</sup>.

The QD spin eigen-state can be prepared, for example, by optical spin pumping<sup>22,50</sup>. From the above discussions, we see the single-shot QND measurement of single spin can be also used to prepare the spin eigen state and cool the spin via photon detection<sup>48</sup>. From the spin basis state, there are two ways to create the spin superposition state: either via spin-flip Raman transitions<sup>22</sup>, or by performing single spin rotations using nanosecond ESR microwave pulses<sup>23</sup>. Recently, ultrafast optical coherent control of electron spins has been reported in quantum wells on femtosecond time scales<sup>51</sup> and in QDs on picosecond time scales<sup>52,53</sup>, which is much shorter than the QD spin coherence time ( $T_2 \sim \mu$ s). This allows ultrafast  $\pi/2$  spin rotation which is required in our schemes for spin state preparation or spin Hadamard operation.

### IV. ENTANGLE REMOTE SPINS VIA A SINGLE PHOTON

We show here that the photon-spin entangling gate can be used to generate entanglement between remote spins in different cavities via a single photon (see Fig. 4a). In the first  $X^-$ -cavity system, the spin is prepared in the state  $|\psi^s\rangle_1 = \alpha_1|\uparrow\rangle_1 + \beta_1|\downarrow\rangle_1$  and transmission operator is  $\hat{t}_1(\omega)$ ; In the second  $X^-$ -cavity system, the spin is prepared in the state  $|\psi^s\rangle_2 = \alpha_2|\uparrow\rangle_2 + \beta_2|\downarrow\rangle_2$  and transmission operator is  $\hat{t}_2(\omega)$ . Both  $X^-$ -cavity systems work in the strong coupling regime to get high gate fidelity, but the parameters  $g$ ,  $\kappa$ ,  $\kappa_s$ ,  $\omega_c$  and  $\omega_{X^-}$  for this two systems are not necessary to be the same.

A single photon in  $|H\rangle$  polarization passes through the first cavity, then through the second cavity, after which its polarization is checked (see Fig. 4a). The corresponding state transformation is

$$|H\rangle \otimes (\alpha_1|\uparrow\rangle_1 + \beta_1|\downarrow\rangle_1) \otimes (\alpha_2|\uparrow\rangle_2 + \beta_2|\downarrow\rangle_2) \xrightarrow{\hat{t}_{1,2}(\omega)} \frac{t_{10}(\omega)t_{20}(\omega)}{\sqrt{2}} (\alpha_1\alpha_2|R\rangle|\uparrow\rangle_1|\uparrow\rangle_1 + \beta_1\beta_2|L\rangle|\downarrow\rangle_1|\downarrow\rangle_2) \quad (9)$$

By applying the Hadamard gate on the photon state using a polarizing beam splitter, we obtain entangled spin

states

$$|\Phi_{12}^s\rangle = \alpha_1\alpha_2|\uparrow\rangle_1|\uparrow\rangle_2 \pm \beta_1\beta_2|\downarrow\rangle_1|\downarrow\rangle_2 \quad (10)$$

on detecting the photon in the  $|H\rangle$  state (for “+”), or in  $|V\rangle = (|R\rangle - |L\rangle)/\sqrt{2}$  state (for “-”). On setting the coefficients  $\alpha_{1,2}$  and  $\beta_{1,2}$  to  $1/\sqrt{2}$ , we get maximally entangled spin states.

We see the single photon works as a quantum bus to couple or entangle remote spins on demand, but the two spins in two cavities can be slightly different in their transition frequencies. However, if the cavity mode frequency  $\omega_c$  and the  $X^-$  transition frequency  $\omega_{X^-}$  match with the photon frequency  $\omega$  for the two  $X^-$ -cavity systems, the success probability  $|t_{10}(\omega)t_{20}(\omega)|^2/2$  to achieve the spin entanglement can be increased. As discussed earlier, if the side leakage can be made significantly small,  $|t_{10}(\omega)|$  and  $|t_{20}(\omega)|$  can both reach unity and we get the maximal success probability of 50%. But we know for certain we have succeeded in entangling the spins when a photon is detected. The schemes based on quantum interference of emitted photons can generate remote atomic entanglement<sup>54,55</sup>, and could be extended to entangle distant spins<sup>56,57</sup>. However these schemes suffer from low success probability, and require identical atoms or spins<sup>55</sup>. There are also some other schemes based on Faraday rotation<sup>33,58</sup> and the probabilistic schemes based on the dispersive spin-photon interactions<sup>59</sup> using bright coherent light as proposed by van Loock et al and Ladd et al<sup>60</sup>.

The above scheme can be easily extended to generate multi-spin entangled states, such as Greenberger-Horne-Zeilinger (GHZ) states<sup>61</sup> by passing the single photon through all cavities and finally checking the photon polarization. On setting all  $\alpha$ 's and  $\beta$ 's to  $1/\sqrt{2}$ , we get maximally entangled spin GHZ states:

$$|\text{GHZ}^s\rangle_N = \frac{1}{\sqrt{N}}(|\uparrow\rangle_1|\uparrow\rangle_2 \cdots |\uparrow\rangle_N \pm |\downarrow\rangle_1|\downarrow\rangle_2 \cdots |\downarrow\rangle_N) \quad (11)$$

Alternatively, starting from entangled spin pairs, we could build higher-order entangled spin states such as GHZ states or cluster states<sup>62</sup> with N unlimited. The success probability is  $1/2^k$  depending on the number k of single photons used. Again the detection of the photons heralds a successful entanglement operation.

We point out here that the influence of photon reflection between cavities can be removed by utilizing suitable timing system. Once we have created entangled spin states, either optical or electrical pumping can be used to excite  $X^-$  in QDs. Spin entanglement is then transferred to photon polarization entanglement via  $X^-$  emissions due to the same optical spin selection rule of  $X^-$  as discussed earlier. However, we show another scheme below - a photon entangler which can entangle independent photons with different frequencies or different pulse length.

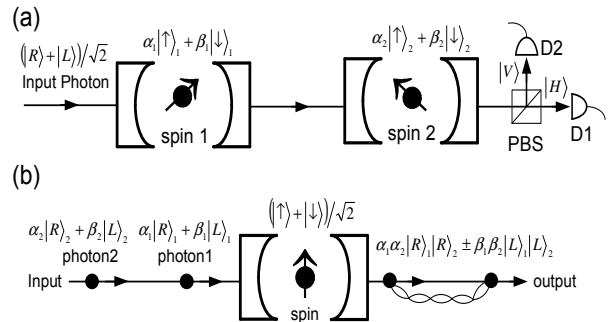


FIG. 4: Schematic diagram of a spin / photon entangler. (a) A proposed scheme to entangle remote spins in different microcavities via a single photon. PBS (polarizing beam splitter) and D1 and D2 (photon detectors). (b) A proposed scheme to entangle independent photons via a single spin in a microcavity.

## V. ENTANGLE INDEPENDENT PHOTONS VIA A SINGLE SPIN

As shown in Fig. 4b, photon 1 in the state  $|\psi^{ph}\rangle_1 = \alpha_1|R\rangle_1 + \beta_1|L\rangle_1$  and photon 2 in the state  $|\psi^{ph}\rangle_2 = \alpha_2|R\rangle_2 + \beta_2|L\rangle_2$  are input into the cavity in sequence. The two independent photons can have different frequencies, but both are in the frequency window  $|\omega - \omega_c| < \kappa$ . The electron spin is prepared in a superposition state  $|\psi^s\rangle = \frac{1}{\sqrt{2}}(|\uparrow\rangle + |\downarrow\rangle)$ . The transmission operator  $\hat{t}(\omega)$  for the  $X^-$ -cavity system is again described by equation (5).

After transmission, the state transformation is

$$\begin{aligned} & (\alpha_1|R\rangle_1 + \beta_1|L\rangle_1) \otimes (\alpha_2|R\rangle_2 + \beta_2|L\rangle_2) \otimes |\psi^s\rangle \\ & \xrightarrow{\hat{t}(\omega)} \frac{t_0(\omega_1)t_0(\omega_2)}{\sqrt{2}} (\alpha_1\alpha_2|R\rangle_1|R\rangle_2|\uparrow\rangle + \beta_1\beta_2|L\rangle_1|L\rangle_2|\downarrow\rangle). \end{aligned} \quad (12)$$

By applying a Hadamard gate on the electron spin (e.g., using a  $\pi/2$  microwave or optical pulse), the right side of equation (12) becomes

$$\begin{aligned} & \frac{t_0(\omega_1)t_0(\omega_2)}{2} \{ (\alpha_1\alpha_2|R\rangle_1|R\rangle_2 + \beta_1\beta_2|L\rangle_1|L\rangle_2)|\uparrow\rangle \\ & + (\alpha_1\alpha_2|R\rangle_1|R\rangle_2 - \beta_1\beta_2|L\rangle_1|L\rangle_2)|\downarrow\rangle \} \end{aligned} \quad (13)$$

Next, the electron spin eigen-state can be detected by the QND measurement as discussed earlier using a weak coherent light (or single photons) in H polarization. Depending on the detected spin state in  $|\uparrow\rangle$  or  $|\downarrow\rangle$ , we get the entangled photon states

$$|\Phi_{12}^{ph}\rangle = (\alpha_1\alpha_2|R\rangle_1|R\rangle_2 \pm \beta_1\beta_2|L\rangle_1|L\rangle_2) \quad (14)$$

On setting the coefficients  $\alpha_{1,2}$  and  $\beta_{1,2}$  to  $1/\sqrt{2}$ , maximally entangled photon states can be generated.

Although photon 1 and photon 2 never meet before, each of them gets entangled with the electron spin after sequentially interacting with the spin. The spin measurement then projects the two photons into entangled states. This entanglement-by-projection scheme does not require photon indistinguishability or photon interference as demanded by other schemes using photon mixing on a beam splitter<sup>63</sup>. This kind of single-photon pulses can come from QD single photon sources<sup>16,17,18</sup>.

Recent experiments have shown GaAs or In(Ga)As single QDs have long electron spin coherence time ( $T_2 \sim \mu\text{s}$ )<sup>23,24</sup> and spin relaxation time ( $T_1 \sim \text{ms}$ )<sup>25</sup>. Due to the spin decoherence, the density matrix of the electron spin in the initial state  $|\psi^s\rangle = \frac{1}{\sqrt{2}}(|\uparrow\rangle + |\downarrow\rangle)$  evolves at time  $t$  ( $t \ll T_1$ )

$$\rho(t) = \begin{pmatrix} 1/2 & e^{-t/T_2}/2 \\ e^{-t/T_2}/2 & 1/2 \end{pmatrix}, \quad (15)$$

which represents a spin mixed state. As a result, the entanglement fidelity with respect to equation (14) becomes

$$F = \frac{1}{2}(1 + e^{-t/T_2}), \quad (16)$$

which decreases with  $t$ . Therefore high fidelity photon entanglement can only be achieved when the time interval between two photons is much shorter than the spin coherence time ( $T_2 \sim \mu\text{s}$ ) in the QD. This entanglement between photons with different arrival time is ideal for quantum relay type applications.

If increasing  $|t_0(\omega)|$  to one by optimizing the cavity, the success probability for the photon entanglement generation can reach 25%, so coincidence measurement of photons is required to post-select the entangled state.

We could also extend this scheme to generate multi-photon GHZ states by passing all photons through the cavity in sequence and finally checking the spin state after applying a Hadamard gate on the spin. An alternative way to generate GHZ<sup>61</sup> or cluster states<sup>62</sup> is to start from the generation of entangled photon pairs and then repeat this procedure to increase the size such that the photon number  $N$  can be unlimited. On setting all  $\alpha$ 's and  $\beta$ 's to  $1/\sqrt{2}$ , we get maximally entangled photon GHZ states:

$$|\text{GHZ}^{ph}\rangle_N = \frac{1}{\sqrt{N}}(|R\rangle_1|R\rangle_2 \cdots |R\rangle_N \pm |L\rangle_1|L\rangle_2 \cdots |L\rangle_N). \quad (17)$$

The maximal success probability is then  $1/2^N$ .

## VI. PHOTON-SPIN QUANTUM INTERFACE

Quantum interface is a critical component for quantum networks. Here we show reversible and coherent quantum-state transfer between photon and spin using the photon-spin entangling gate. In Fig. 5a, a photon in an arbitrary state  $|\psi^{ph}\rangle = \alpha|R\rangle + \beta|L\rangle$  is input to

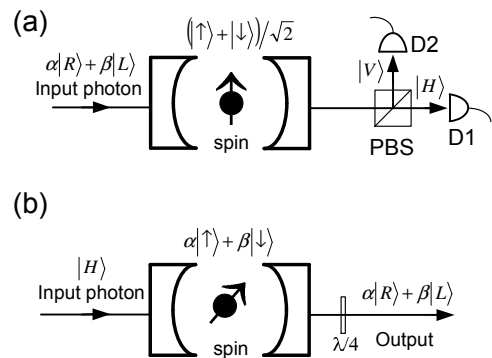


FIG. 5: Schematic diagram of a photon-spin quantum interface. (a) State transfer from a photon to a spin. (b) State transfer from a spin to a photon. PBS (polarizing beam splitter), D1 and D2 (photon detectors), and  $\lambda/4$  (quarter-wave plate).

the cavity with the electron spin prepared in the state  $|\psi^s\rangle = \frac{1}{\sqrt{2}}(|\uparrow\rangle + |\downarrow\rangle)$ . After transmission, the photon and the spin become entangled, i.e.,

$$(\alpha|R\rangle + \beta|L\rangle) \otimes |\psi^s\rangle \xrightarrow{i(\omega)} \frac{t_0(\omega)}{\sqrt{2}} (\alpha|R\rangle|\uparrow\rangle + \beta|L\rangle|\downarrow\rangle). \quad (18)$$

By applying a Hadamard gate on the photon state using a polarizing beam splitter, we obtain a spin state  $|\Phi_1^s\rangle = \alpha|\uparrow\rangle \pm \beta|\downarrow\rangle$  on detecting a photon in the  $|H\rangle$  or  $|V\rangle$  state. Therefore, the photon state is transferred to the electron spin state.

In Fig. 5b, a photon in the polarization state  $|\psi^{ph}\rangle = (|R\rangle + |L\rangle)/\sqrt{2}$  is input to the cavity with the electron spin in an arbitrary state  $|\psi^s\rangle = \alpha|\uparrow\rangle + \beta|\downarrow\rangle$ . After transmission, the photon and the spin become entangled, i.e.,

$$|\psi^{ph}\rangle \otimes (\alpha|\uparrow\rangle + \beta|\downarrow\rangle) \xrightarrow{i(\omega)} \frac{t_0(\omega)}{\sqrt{2}} (\alpha|R\rangle|\uparrow\rangle + \beta|L\rangle|\downarrow\rangle). \quad (19)$$

After applying a Hadamard gate on the electron spin (e.g., using a  $\pi/2$  microwave or optical pulse), the spin eigen-state is detected by the QND measurement as discussed earlier. On detecting the electron spin in the  $|\uparrow\rangle$  or  $|\downarrow\rangle$  state, the photon is then projected in the state  $|\Phi_1^{ph}\rangle = \alpha|R\rangle \pm \beta|L\rangle$ . So the spin state is transferred to the photon state.

In contrast to the original teleportation protocol which involves three qubits<sup>64</sup>, our state transfer scheme requires only two qubits thanks to the tunable amount of entanglement. The success probability is  $|t_0(\omega)|^2/2$ , which can be increased to 50% by optimizing the cavity. The state transfer fidelity is determined by the gate fidelity as described by equation (6).

## VII. CONCLUSIONS

Entanglement is a fundamental resource in quantum information science. With the proposed photon-spin entangling gate, it is possible to generate almost all kinds of local or remote entanglement among photons and QD spins with high fidelity. This entanglement would find wide applications in quantum communications such as quantum cryptography and quantum teleportation. Moreover, this entanglement is essential to implement a quantum bus, quantum interface, quantum memories and quantum repeaters, all of which are critical building blocks for quantum networks. The high-order multiparticle entanglement could be used for entanglement-enhanced quantum measurement<sup>65</sup>, or cluster-state based quantum computing<sup>66,67</sup>.

This gate can also work as an active device such as a polarization-controlled single photon source<sup>16,17,18</sup>, which could be driven by the electron spin dynam-

ics. These single photons on demand can be sent back to the gate to get entangled photons based on our schemes. Techniques for manipulating single photons have been well developed, and significant progress on fast QD-spin cooling and manipulating has been made recently<sup>22,23,50,52</sup>. Together with this work, we believe a charged QD in an optical cavity is promising for solid-state quantum networks and quantum computing.

## Acknowledgements

C.Y.H. thanks M. Atatüre, S. Bose, and S. Popescu for helpful discussions. J.G.R. acknowledges support from the Royal Society. This work is partly funded by EPSRC-GB IRC in Quantum Information Processing, QAP (Contract No. EU IST015848), and MEXT from Japan.

- 
- \* Electronic address: chengyong.hu@bristol.ac.uk
- <sup>1</sup> J.I. Cirac, P. Zoller, H.J. Kimble, and H. Mabuchi, Phys. Rev. Lett. **78**, 3221 (1997).
  - <sup>2</sup> A. Kuhn, M. Hennrich, and G. Rempe, Phys. Rev. Lett. **89**, 067901 (2002).
  - <sup>3</sup> J. McKeever, A. Boca, A.D. Boozer, R. Miller, J.R. Buck, A. Kuzmich, and H.J. Kimble, Science **303**, 1992 (2004).
  - <sup>4</sup> T. Wilk, S.C. Webster, H.P. Specht, G. Rempe, and A. Kuhn, Phys. Rev. Lett. **98**, 063601 (2007).
  - <sup>5</sup> J.F. Sherson, H. Krauter, R.K. Olsson, B. Julsgaard, K. Hammerer, I. Cirac, and E.S. Polzik, Nature(London) **443**, 557 (2006).
  - <sup>6</sup> A.D. Boozer, A. Boca, R. Miller, T.E. Northup, and H.J. Kimble, Phys. Rev. Lett. **98**, 193601 (2007).
  - <sup>7</sup> T. Wilk, S.C. Webster, A. Kuhn, and G. Rempe, Science **317**, 488 (2007).
  - <sup>8</sup> A.A. Houck, D.I. Schuster, J.M. Gambetta, J.A. Schreier, B.R. Johnson, J.M. Chow, L. Frunzio, J. Majer, M.H. Devoret, S.M. Girvin, and R.J. Schoelkopf, Nature(London) **449**, 328 (2007).
  - <sup>9</sup> M.A. Sillanpää, J.I. Park, and R.W. Simmonds, Nature(London) **449**, 438 (2007).
  - <sup>10</sup> J. Majer, J.M. Chow, J.M. Gambetta, J. Koch, B.R. Johnson, J.A. Schreier, L. Frunzio, D.I. Schuster, A.A. Houck, A. Wallraff, A. Blais, M.H. Devoret, S.M. Girvin, and R.J. Schoelkopf, Nature(London) **449**, 443 (2007).
  - <sup>11</sup> D. Loss and D.P. DiVincenzo, Phys. Rev. A **57**, 120 (1998).
  - <sup>12</sup> A. Imamoglu, D.D. Awschalom, G. Burkard, D.P. DiVincenzo, D. Loss, M. Sherwin, and A. Small, Phys. Rev. Lett. **83**, 4204 (1999).
  - <sup>13</sup> T. Calarco, A. Datta, P. Fedichev, E. Pazy, and P. Zoller, Phys. Rev. A **68**, 012310 (2003).
  - <sup>14</sup> W. Yao, R.-B. Liu, and L. J. Sham, Phys. Rev. Lett. **95**, 030504 (2005).
  - <sup>15</sup> S.M. Clark, Kai-Mei C. Fu, T.D. Ladd, and Y. Yamamoto, Phys. Rev. Lett. **99**, 040501 (2007).
  - <sup>16</sup> E. Moreau, I. Robert, J.M. Gérard, I. Abram, L. Manin, and V. Thierry-Mieg, Appl. Phys. Lett. **79**, 2865 (2001).
  - <sup>17</sup> Z. L. Yuan, B. E. Kardynal, R. M. Stevenson, A. J. Shields, C. J. Lobo, K. Cooper, N. S. Beattie, D. A. Ritchie, and M. Pepper, Science **295**, 102 (2002).
  - <sup>18</sup> C. Santori, D. Fattal, J. Vuckovic, G.S. Solomon, and Y. Yamamoto, Nature(London) **419**, 594 (2002).
  - <sup>19</sup> R. M. Stevenson, R. J. Young, P. Atkinson, K. Cooper, D. A. Ritchie, and A. J. Shields, Nature (London) **439**, 179 (2006).
  - <sup>20</sup> N. Akopian, N.H. Lindner, E. Poem, Y. Berlatzky, J. Avron, D. Gershoni, B.D. Gerardot, and P.M. Petroff, Phys. Rev. Lett. **96**, 130501 (2006).
  - <sup>21</sup> D.D. Awschalom, D. Loss, and N. Samarth, *Semiconductor Spintronics and Quantum Computation* (Springer-Verlag, New York, 2002).
  - <sup>22</sup> M. Atatüre, J. Dreiser, A. Badolato, A. Hogege, K. Karrai, and A. Imamoglu, Science **312**, 551 (2006).
  - <sup>23</sup> J. R. Petta, A. C. Johnson, J. M. Taylor, E. A. Laird, A. Yacoby, M. D. Lukin, C. M. Marcus, M. P. Hanson, and A. C. Gossard, Science **309**, 2180 (2005)
  - <sup>24</sup> A. Greilich, D. R. Yakovlev, A. Shabaev, Al. L. Efros, I.A. Yugova, R. Oulton, V. Stavarache, D. Reuter, A. Wieck, and M. Bayer, Science **313**, 341 (2006).
  - <sup>25</sup> J. M. Elzerman, R. Hanson, L. H. Willems van Beveren, B. Witkamp, L. M. K. Vandersypen, and L. P. Kouwenhoven, Nature (London) **430**, 431(2004); M. Kroutvar, Y. Ducommun, D. Heiss, M. Bichler, D. Schuh, G. Abstreiter, and J. J. Finley, Nature (London) **432**, 81 (2004).
  - <sup>26</sup> J.P. Reithmaier, G. Şek, A. Löffler, C. Hofmann, S. Kuhn, S. Reitzenstein, L. V. Keldysh, V. D. Kulakovskii, T. L. Reinecke, A. Forchel, Nature **432**, 197 (2004).
  - <sup>27</sup> T. Yoshie, A. Scherer, J. Hendrickson, G. Khitrova, H. M. Gibbs, G. Rupper, C. Ell, O. B. Shchekin, D.G. Deppe, Nature **432**, 200 (2004).
  - <sup>28</sup> E. Peter, P. Senellart, D. Martrou, A. Lemaître, J. Hours, J. M. Gérard, and J. Bloch, Phys. Rev. Lett. **95**, 067401 (2005).
  - <sup>29</sup> K. Hennessy, A. Badolato, M. Winger, D. Gerace, M. Atatüre, S. Gulde, S. Fält, E.L. Hu, and A. Imamoglu,

- Nature(London) **445**, 896 (2007).
- <sup>30</sup> D. Press, S. Götzinger, S. Reitzenstein, C. Hofmann, A. Löffler, M. Kamp, A. Forchel, and Y. Yamamoto, Phys. Rev. Lett. **98**, 117402 (2007).
  - <sup>31</sup> S. Reitzenstein, C. Hofmann, A. Gorbunov, M. Strauß, S. H. Kwon, C. Schneider, A. Löffler, S. Höfing, M. Kamp, and A. Forchel, Appl. Phys. Lett. **90**, 251109 (2007).
  - <sup>32</sup> Christian Flindt, Anders S. Sørensen, Mikhail D. Lukin, and Jacob M. Taylor, Phys. Rev. Lett. **98**, 240501 (2007).
  - <sup>33</sup> C.Y. Hu, A. Young, J. L. O'Brien, W. J. Munro, and J. G. Rarity, Phys. Rev. B **78**, 085307 (2008).
  - <sup>34</sup> C.Y. Hu, W.J. Munro, and J.G. Rarity, Phys. Rev. B **78**, 125318 (2008).
  - <sup>35</sup> R.J. Warburton, C.S. Dürr, K. Karrai, J. P. Kotthaus, G. Medeiros-Ribeiro, and P. M. Petroff, Phys. Rev. Lett. **79**, 5282 (1997).
  - <sup>36</sup> C.Y. Hu, W. Ossau, D. R. Yakovlev, G. Landwehr, T. Wojtowicz, G. Karczewski, and J. Kossut, Phys. Rev. B **58**, R1766 (1998).
  - <sup>37</sup> D.F. Walls and G.J. Milburn, *Quantum Optics* (Springer-Verlag, Berlin, 1994).
  - <sup>38</sup> E. Waks, and J. Vučković, J. Phys. Rev. Lett. **96**, 153601 (2006).
  - <sup>39</sup> A. AUFFEVES-GARNIER, C. Simon, C. Gerard, and J. Poizat, Phys. Rev. A **75**, 053823 (2007).
  - <sup>40</sup> D. Englund, D. Fattal, E. Waks, G. Solomon, B. Zhang, T. Nakaoka, Y. Arakawa, Y. Yamamoto, and J. Vučković, Nature(London) **450**, 857 (2007).
  - <sup>41</sup> G. Bester, S. Nair, and A. Zunger, Phys. Rev. B **67**, 161306(R) (2003).
  - <sup>42</sup> For a review, see e.g., A.J. Shields, Nature Photonics **1**, 215 (2007).
  - <sup>43</sup> Q.A. Turchette, C.J. Hood, W. Lange, H. Mabuchi, and H.J. Kimble, Phys. Rev. Lett. **75**, 4710 (1995).
  - <sup>44</sup> N.H. Lindner and T. Rudolph, eprint: quant-ph/0810.2587.
  - <sup>45</sup> P. Grangier, J.A. Levenson, and J.P. Poizat, Nature(London) **396**, 537 (1998).
  - <sup>46</sup> J. Berezovsky, M.H. Mikkelsen, O. Gywat, N. G. Stoltz, L. A. Coldren, and D. D. Awschalom, Science **314**, 1916 (2006).
  - <sup>47</sup> M. Atatüre, J. Dreiser, A. Badolato, and A. Imamoglu, Nature Physics **3**, 101 (2007).
  - <sup>48</sup> R.B. Liu, W. Yao, and L.J. Sham, Phys. Rev. B **72**, 081306 (2005).
  - <sup>49</sup> K. Nemoto and W.J. Munro, Phys. Lett. A **344**, 104 (2005).
  - <sup>50</sup> Xiaodong Xu, Yanwen Wu, Bo Sun, Qiong Huang, Jun Cheng, D. G. Steel, A. S. Bracker, D. Gammon, C. Emary, and L. J. Sham, Phys. Rev. Lett. **99**, 097401 (2007).
  - <sup>51</sup> J.A. Gupta, R. Knobel, N. Samarth, and D. D. Awschalom, Science **292**, 2458 (2001).
  - <sup>52</sup> J. Berezovsky, M. H. Mikkelsen, N. G. Stoltz, L. A. Coldren, and D.D. Awschalom, Science **320**, 349 (2008).
  - <sup>53</sup> David Press, Thaddeus D. Ladd, Bingyang Zhang, Yoshihisa Yamamoto, Nature (London) **456**, 218 (2008).
  - <sup>54</sup> C.W. Chou, H. de Riedmatten, D. Felinto, S.V. Polyakov, S.J. van Enk, and H. J. Kimble, Nature(London) **438**, 828 (2005).
  - <sup>55</sup> D.L. Moehring, P. Maunz, S. Olmschenk, K.C. Younge, D.N. Matsukevich, L.M. Duan, and C. Monroe, Nature (London) **449**, 68 (2007).
  - <sup>56</sup> L. Childress, J.M. Taylor, A.S. Sørensen, and M.D. Lukin, Phys. Rev. Lett. **96**, 070504 (2006).
  - <sup>57</sup> C. Simon, Y.M. Niquet, X. Caillet, J. Eymery, J.P. Poizat, and J.M. Gérard, Phys. Rev. B **75**, 081302(R) (2007).
  - <sup>58</sup> M.N. Leuenberger, M.E. Flatté, and D. D. Awschalom, Phys. Rev. Lett. **94**, 107401 (2005).
  - <sup>59</sup> Julian Grond, Walter Pötz, and Atac Imamoglu, Phys. Rev. B **77**, 165307 (2008).
  - <sup>60</sup> P. van Loock, T.D. Ladd, K. Sanaka, F. Yamaguchi, K. Nemoto, W.J. Munro, and Y. Yamamoto, Phys. Rev. Lett. **96**, 240501 (2006); T.D. Ladd, P. van Loock, K. Nemoto, W.J. Munro, and Y. Yamamoto, New J. Phys. **8**, 184 (2006).
  - <sup>61</sup> M. Greenberger, M.A. Horne, A. Shimony, and A. Zeilinger, Am. J. Phys. **58**, 1131 (1990).
  - <sup>62</sup> H.J. Briegel and R. Raussendorf, Phys. Rev. Lett. **86**, 910 (2001).
  - <sup>63</sup> D. Fattal, K. Inoue, J. Vučković, C. Santori, G. S. Solomon, and Y. Yamamoto, Phys. Rev. Lett. **92**, 037903 (2004); D. Fattal, E. Diamanti, K. Inoue, and Y. Yamamoto, Phys. Rev. Lett. **92**, 037904 (2004).
  - <sup>64</sup> C.H. Bennett, G. Brassard, C. Crépeau, R. Jozsa, A. Peres, and W.K. Wootters, Phys. Rev. Lett. **70**, 1895 (1993).
  - <sup>65</sup> V. Giovannetti, S. Lloyd, and L. Maccone, Science **306**, 1330 (2004).
  - <sup>66</sup> R. Raussendorf and H.J. Briegel, Phys. Rev. Lett. **86**, 5188 (2001).
  - <sup>67</sup> M.A. Nielsen, Rev. Math. Phys. **57**, 147 (2006).